Article

Not peer-reviewed version

Optimizing Tempering Parameters to Enhance Precipitation Behavior and Impact Toughness in High-Nickel Steel

Guojin Sun * and Qi Wang

Posted Date: 16 July 2024

doi: 10.20944/preprints202407.1112.v1

Keywords: Tempering process; Precipitation; High-nickel steel; Impact toughness; EBSD

 doi:10.20944/preprints202407.1112.v1

Article

Optimizing Tempering Parameters to Enhance Precipitation Behavior and Impact Toughness in High-Nickel Steel

Guojin Sun [1,*] and Qi Wang [2]

[1] School of Engineering, Qinghai Institute of Technology, Xining 810016, China
[2] Electrical Engineering Division, Department of Engineering, University of Cambridge, Cambridge CB3 0FA, UK
* Correspondence: sunguojin1982@126.com

Abstract: This study explores the effects of tempering on the precipitation behavior and impact toughness of high-nickel steel. The specimens underwent double quenching at 870°C and 770°C, followed by tempering at various temperatures. Advanced characterization techniques including optical microscopy (OM), scanning electron microscopy (SEM), and transmission electron microscopy (TEM) were used to elucidate precipitation phenomena. Additionally, electron backscatter diffraction (EBSD) was employed to assess the misorientation distribution after tempering. Charpy impact tests were performed on specimens tempered at different temperatures to evaluate their toughness. The findings reveal that with increasing tempering temperature, the fraction of low-angle grain boundaries decreases, which correlates positively with enhanced impact toughness. The impact toughness peaks at 580°C and then diminishes with further temperature increases.

Keywords: tempering process; precipitation; high-nickel steel; impact toughness; EBSD

1. Introduction

High-strength alloy steels are extensively used in applications such as springs, stabilizers, and ship structures due to their exceptional ability to meet specific design requirements, including high strength, impact toughness, and low ductile-to-brittle transition temperatures [1–4]. The mechanical properties and microstructures of these steels can be significantly enhanced through heat treatment processes, with tempering being one of the most critical treatments Over the past decades, extensive research has focused on the role of tempering in modifying precipitation behavior and improving the mechanical properties of steels[5–8].

Tempering involves heating the steel to a temperature below its critical point, followed by cooling, to achieve desired mechanical properties through various transformation mechanisms. These mechanisms, which involve either long-range or short-range atomic transport, can be categorized into distinct stages based on microstructural evolution. The first stage of tempering (100-200°C) involves the precipitation of ε-carbides. These carbides nucleate due to modulated structures formed during low-temperature aging, and at the end of this stage, martensite retains its tetragonality. In low-carbon steels, this stage may not be prominent due to limited ε-carbide formation[9]. The second stage (200-300°C) is characterized by the decomposition of residual austenite into ferrite and cementite, driven by carbon diffusion in the austenite. During the third stage (200-350°C), cementite appears with a Widmanstätten distribution, characterized by a specific orientation relationship with the matrix. In the fourth stage (400-700°C), cementite particles coarsen and lose their crystallographic morphology, and martensite lath boundaries are replaced by equiaxed ferrite grain boundaries[10–14].

 doi:10.20944/preprints202407.1112.v1

The addition of alloying elements to steel significantly influences the tempering process. These elements can retard the growth of carbides and preserve the supersaturation of the α-solution with carbon, maintaining the state of tempered martensite up to 400-500°C. Furthermore, alloying elements can slow down recrystallization and polygonization processes, further affecting the tempering outcomes[15–20].

Characterizing misorientation in metals is crucial because it impacts mechanical properties at various temperatures, as well as physical properties, surface properties, and phase transformations. Misorientation analysis, now effectively performed using electron backscatter diffraction (EBSD), provides valuable insights into microstructural features[21–23]. EBSD has become an indispensable tool in materials science, particularly for steel microstructure characterization, due to its ability to provide detailed orientation mapping at high spatial resolutions. This technique allows researchers to investigate grain boundary characteristics, phase distributions, and deformation mechanisms in a wide range of metallic materials[24–27]. One of the primary advantages of EBSD is its ability to generate orientation maps that reveal the crystallographic orientation of grains within a polycrystalline material. These maps are essential for understanding the relationships between processing conditions, microstructure, and mechanical properties. EBSD's high sensitivity to small misorientations enables the detection of subtle changes in grain structure and the identification of low-angle grain boundaries, which are critical for predicting material performance under various loading conditions. By analyzing misorientation between lattices—expressed by rotation axes and angles—researchers can gain a comprehensive understanding of the roles of different phases in forming microstructures [28–30]. The ability to correlate misorientation data with mechanical properties makes EBSD an essential technique for developing advanced high-strength steels with improved performance characteristics.

Although the precipitation processes during quenching and tempering in nickel alloy steels have been widely studied, detailed investigations, particularly in steels with around 4.5% nickel, remain insufficient. This study aims to investigate the influence of tempering temperature on the impact toughness of high-nickel steel. By utilizing OM, SEM, and TEM, the precipitation behavior during the tempering process is elucidated. Additionally, EBSD is employed to reveal misorientation distributions and their impact on the steel's toughness.

2. Experimental

The main chemical composition of the high-nickel alloy steels studied is presented in Table 1. Cuboid samples with dimensions of 150 mm × 80 mm × 20 mm were machined from the steel plate for subsequent heat treatment processes. The experimental procedure included double quenching from 870°C and 770°C followed by tempering at various temperatures to achieve different misorientation distributions. The schematic representation of the heat treatment procedures is depicted in Figure 1, where the x-axis denotes the soaking time and the y-axis represents the temperature.

Table 1. Chemical composition of the high-nickel alloy steel (wt.%).

Element	C	Si	Ni	P	Si	S	Mn	Cr	Cu	V	Mo
Content	0.1	0.2	4.5	0.01	0.25	0.01	0.5	1.5	0.2	0.06	0.5

 doi:10.20944/preprints202407.1112.v1

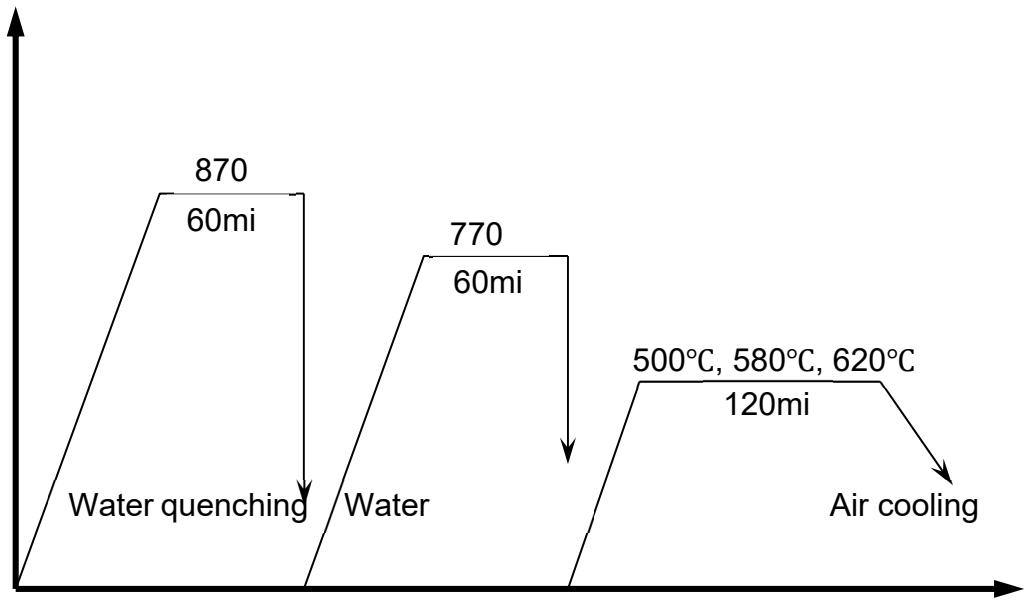

Figure 1. Schematic representation of the heat treatment procedures.

After heat treatment, V-notch Charpy impact specimens with dimensions of 10 mm × 10 mm × 55 mm (as shown in Figure 2) were machined from the steel plates. The Charpy impact tests were conducted at -20°C to evaluate the impact toughness of the specimens.

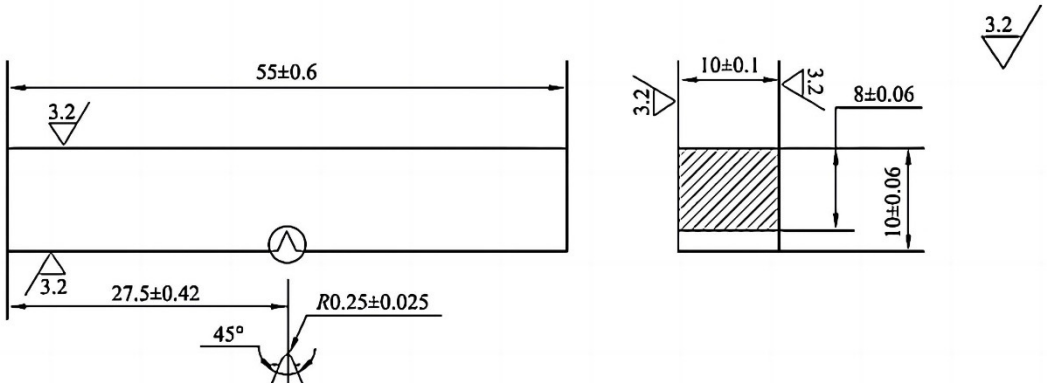

Figure 2. Standard Charpy impact specimen.

To analyze the microstructural characteristics and misorientation distributions post-tempering, a range of advanced microscopy techniques were employed. Electron backscatter diffraction (EBSD) was used to detect the misorientation distributions within the steel. Additionally, optical microscopy (OM), scanning electron microscopy (SEM), and transmission electron microscopy (TEM) were utilized to perform detailed microstructural characterizations. These techniques were crucial for revealing the precipitation behavior and calculating the sizes of the precipitation particles.

3. Results and Discussions

Tempering at temperatures below the Ac1 is a critical step in heat treatment, affecting the redistribution or precipitation of carbon and alloying elements as carbides depending on the tempering temperature, which in turn enhances the mechanical properties of steels. During tempering, the dislocation density decreases, and residual stresses from quenching are relieved. This section presents the detailed results of the microstructural and mechanical property analyses performed on the high-nickel steel after tempering at various temperatures. Figure 1 shows the SEM microstructures at various tempering temperatures.

 doi:10.20944/preprints202407.1112.v1

After tempering for 2 hours, fine carbides precipitate, as observed in Figure 3b–d for tempering temperatures of 500°C, 580°C, and 620°C, respectively. At 500°C, the microstructure shows a significant number of fine carbides distributed within the martensitic matrix, predominantly precipitating along the lath boundaries and within the laths. This distribution is critical in enhancing the steel's hardness and wear resistance. Cementite particles precipitate within the martensite and along lath orientations, contributing to the overall hardness and stability of the microstructure.

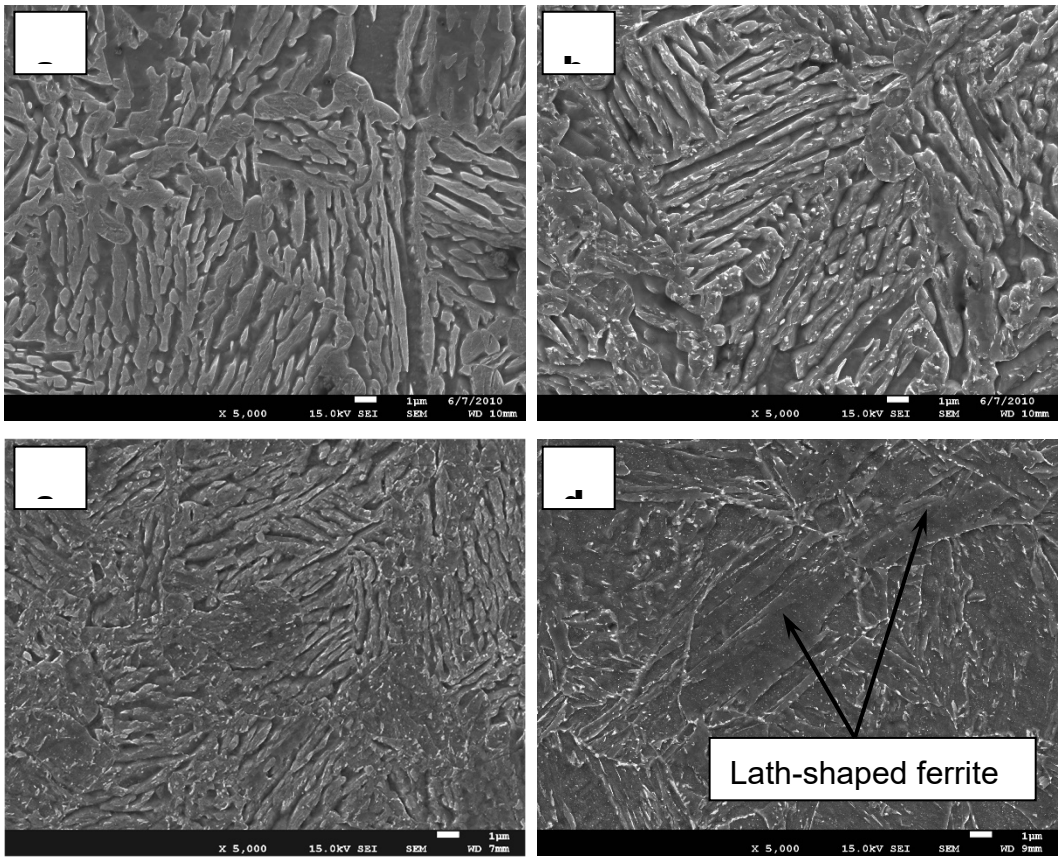

Figure 3. SEM images of steel at various tempering temperatures (a) As-quenched; (b) 500°C; (c) 580°C; (d) 620°C.

The addition of alloying elements, such as nickel and molybdenum, significantly affects the precipitation behavior during tempering. These elements play a crucial role in stabilizing the carbides and preventing their coarsening. Notably, tempering at 580°C results in fine precipitates without significant coarsening, attributable to the segregation of alloying elements at the carbide-ferrite interface. This segregation acts as a barrier to carbon diffusion, thereby maintaining the fine precipitate size and ensuring a uniform distribution throughout the matrix. The presence of alloying elements in the cementite structure inhibits its coarsening during the fourth stage of tempering. This inhibition is particularly beneficial as it helps maintain the mechanical properties of the steel, such as toughness and hardness, over extended periods.

Although martensite lath boundaries remain stable up to approximately 620°C, considerable dislocation rearrangement occurs within the laths. This rearrangement reduces dislocation density and leads to the formation of lath-shaped ferrite grains derived from martensite, as indicated in Figure 3d. At 620°C, the microstructure undergoes more pronounced changes. The precipitates begin to coarsen significantly, and the martensitic laths transform into equiaxed ferrite grains. This transformation is accompanied by a decrease in hardness and an increase in toughness, as the steel's microstructure becomes more stable and less prone to brittle fracture.

Figure 4 presents the misorientation distributions after tempering at 500°C, 580°C, and 620°C. And Figure 5 displays the misorientation angles within a single grain.

Preprints.org (www.preprints.org) | NOT PEER-REVIEWED | Posted: 16 July 2024 doi:10.20944/preprints202407.1112.v1

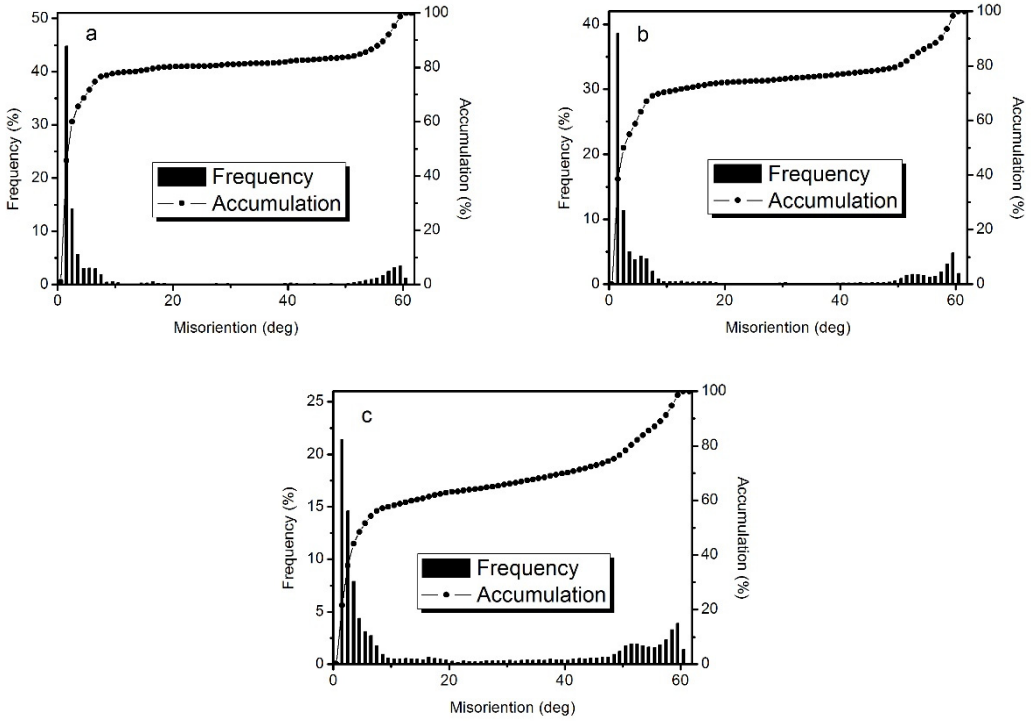

Figure 4. Misorientation distribution at different tempering temperatures (a)500℃; (b) 580℃; (b) 620℃.

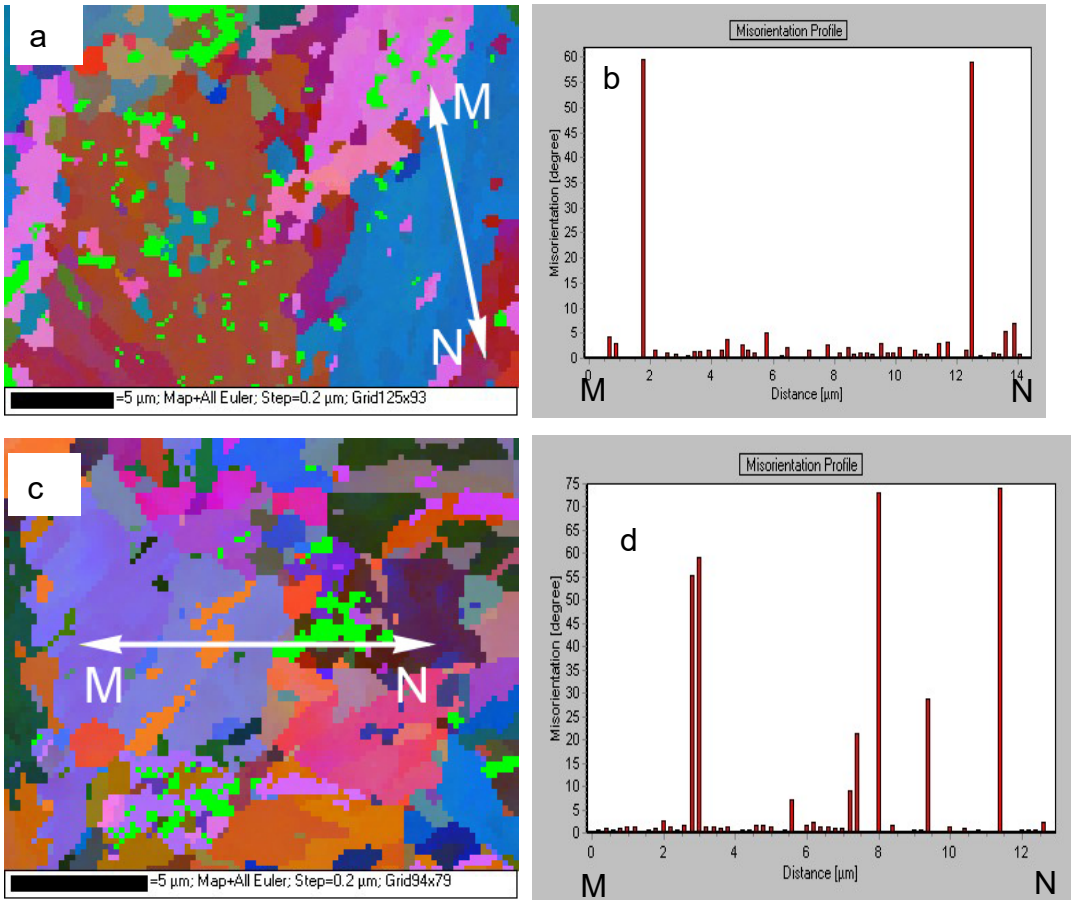

Figure 5. Misorientation distribution within grains at different tempering temperatures. (a) and (b) at 500℃; (c) and (d) at 620℃.

 doi:10.20944/preprints202407.1112.v1

As the tempering temperature increases, low-angle boundaries decrease, as shown in Figure 4. At 500°C, low-angle boundaries (angles less than 10°) exceed 75%, indicating a high density of dislocations and sub-grain boundaries, which contribute to the material's strength but also to its brittleness. At 580°C, low-angle boundaries decrease to about 70%, indicating that precipitation particles lose their orientations. This reduction in low-angle boundaries is beneficial, as it leads to a more random distribution of precipitates, which enhances the mechanical properties, particularly impact toughness. The random distribution helps to interrupt crack propagation pathways, thereby increasing the material's ability to absorb impact energy. At 620°C, low-angle boundaries further decrease, leading to coarsened precipitates as finer particles dissolve into the matrix to support the growth of larger particles.

This coarsening effect is significant as it indicates the movement and redistribution of alloying elements within the microstructure, which impacts the overall toughness and ductility of the steel. Figure 5 shows that at 500°C, misorientation angles within a grain do not exceed 5°, suggesting a relatively uniform strain distribution within the grains. However, at 620°C, misorientation angles range from 5° to 12°, suggesting a more heterogeneous strain distribution. These higher misorientation angles absorb less energy and provide minimal resistance to crack propagation, which can lead to reduced toughness. This indicates that while tempering at higher temperatures can reduce residual stresses and dislocation densities, it can also introduce larger grain boundary misorientations that might detract from the material's overall toughness and impact resistance.

The evolution of precipitation with increasing tempering temperature is shown in Figure 6.

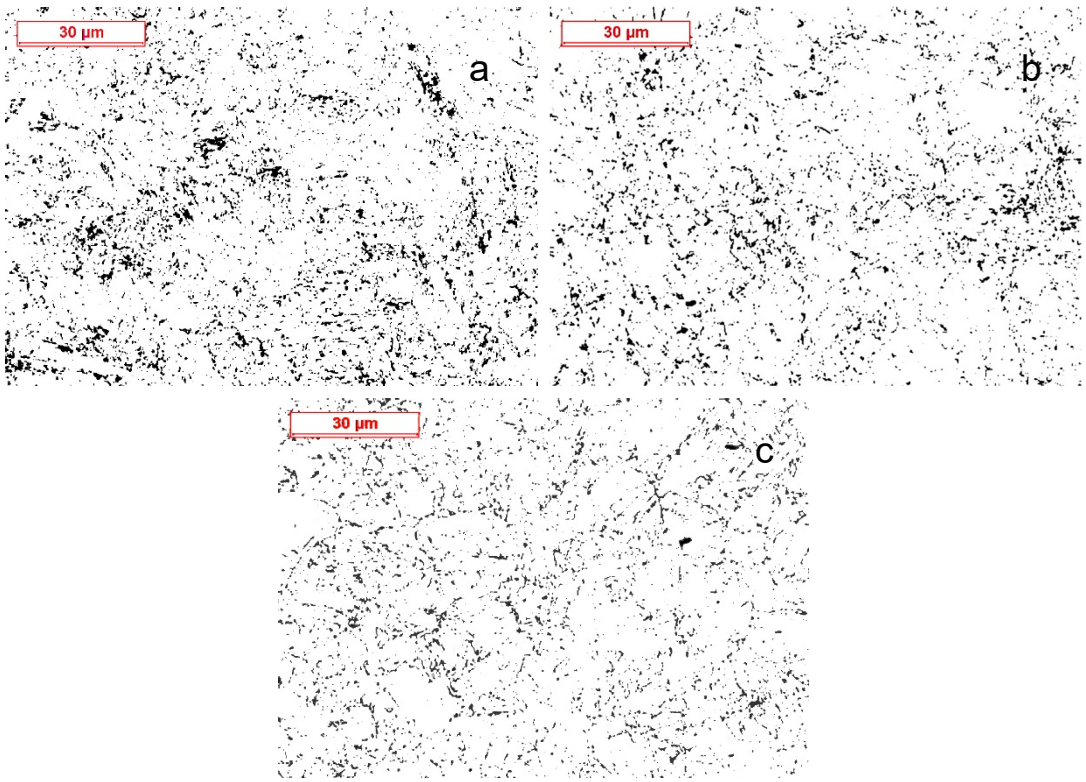

Figure 6. Precipitation distribution at various tempering temperature: (a) 500°C;(b) 580°C;(c) 620°C.

From Figure 6 it can be seen that the number of precipitates decreases slightly as the tempering temperature rises. At 500°C, precipitates typically follow a Widmanstätten distribution, characterized by a specific crystallographic orientation. By 580°C, precipitates lose their distinct crystallographic morphology due to reduced dislocations and the onset of spheroidization, where smaller precipitates begin to dissolve into the matrix. This dissolution provides carbon and alloying elements for the selective growth of larger particles. At 620°C, this phenomenon becomes more pronounced. The increased temperature accelerates the diffusion rates of carbon and alloying elements, leading to significant coarsening of precipitates. Smaller particles dissolve, contributing to the growth of larger

 doi:10.20944/preprints202407.1112.v1

precipitates, which now dominate the microstructure. This coarsening results in a more homogeneous distribution throughout the matrix, which can influence the steel's mechanical properties. The changes in precipitate size and distribution are crucial for understanding the impact of tempering temperature on the material's performance, particularly its impact toughness and strength.

TEM images of steel after tempering are shown in Figure 7, offering more detailed insights than SEM and OM.

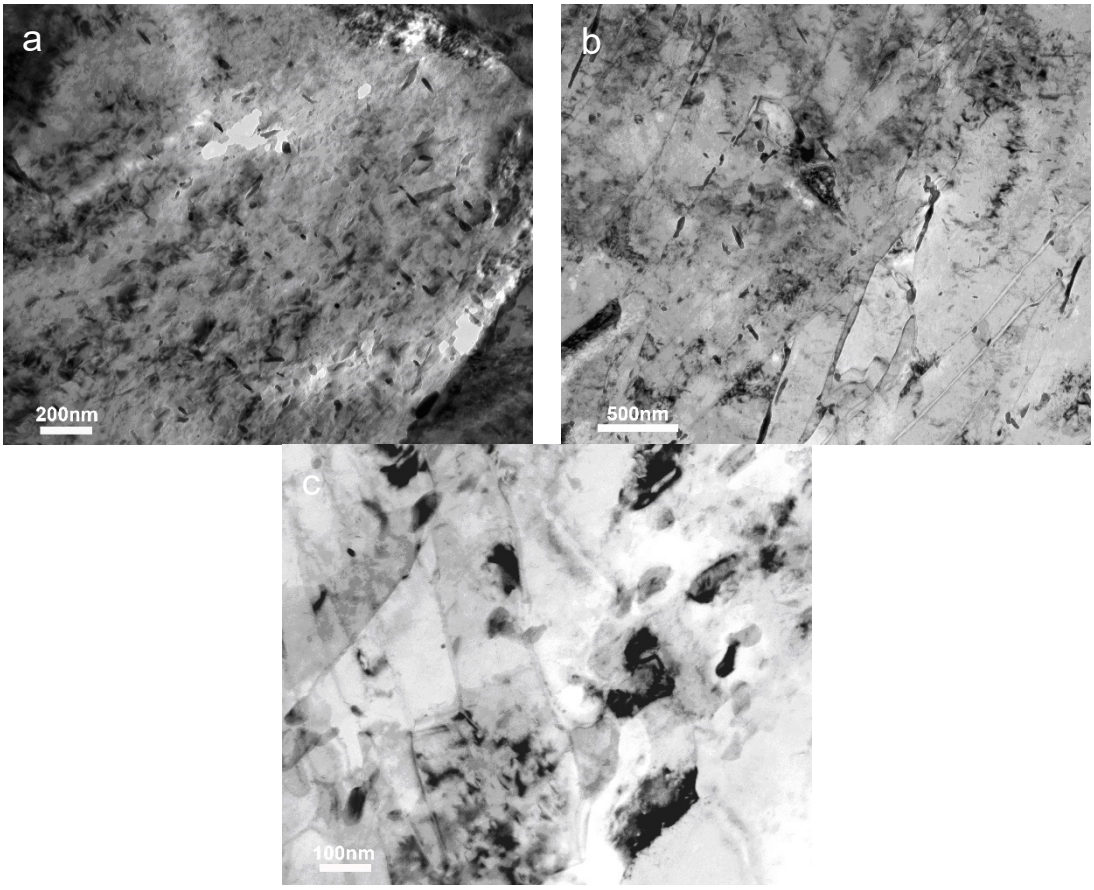

Figure 7. TEM images of steel at various tempering temperatures. (a) 500°C;(b) 580°C;(c) 620°C.

Fine carbides precipitate during tempering, significantly influenced by temperature. At lower temperatures, carbides precipitate along specific orientations, as shown in Figure 7a. At 580°C, precipitates lose their orientations (Figure 7b), and at 620°C, they completely lose orientation (Figure 7c), distributing along lath-shaped ferrite grain boundaries derived from martensite. Carbide nucleation sites include various boundaries, dislocations, and within grains, driven by the diffusion of carbon and alloying elements, with boundaries or dislocations providing rapid diffusion paths.

Figure 8 shows the precipitation size distribution as a function of tempering temperature. At 500°C, precipitation sizes follow a approximately normal distribution, with most precipitates smaller than 20 nm (Figure 8a). At 580°C, the average precipitation size increases to about 25 nm without significant coarsening (Figure 8b). However, at 620°C, a notable coarsening effect occurs, as evidenced by a marked increase in the size of the precipitates. Smaller precipitates dissolve and their material diffuses, leading to the growth of larger particles, which is indicated by a second peak in the distribution curve (Figure 8c).

 doi:10.20944/preprints202407.1112.v1

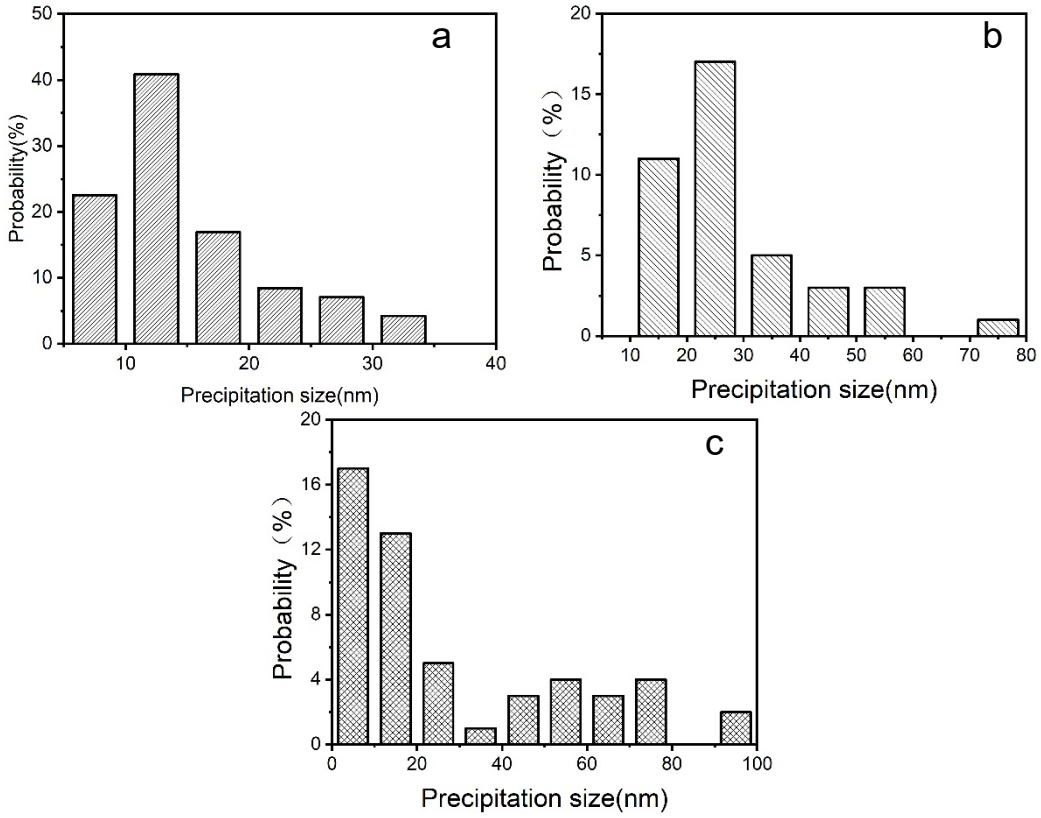

Figure 8. Precipitation size distribution curves at different tempering temperatures (a) 500°C; (b) 580°C; (c) 620°C.

The TEM results reveal that at lower tempering temperatures, such as 500°C, the carbides precipitate predominantly along the martensite lath boundaries and within the laths themselves, forming a relatively ordered and oriented distribution. As the tempering temperature increases to 580°C, the carbides begin to lose their sharp orientation and start to distribute more randomly within the ferrite grains, as the dislocation density decreases and the carbides spheroidize. This random distribution enhances the impact toughness of the steel by reducing the stress concentration points and providing more uniform mechanical properties.

At the highest tempering temperature of 620°C, the carbides become fully spheroidized and lose their initial orientation completely. They are now predominantly located along the lath-shaped ferrite grain boundaries, indicating significant coarsening. The increased diffusion rates at this temperature facilitate the growth of larger carbide particles, as smaller particles dissolve and their material diffuses to larger particles. This coarsening effect can be seen clearly in the precipitation size distribution curves in Figure 8, where a noticeable shift towards larger particle sizes is observed at 620°C. This redistribution and growth of carbides play a critical role in the resulting mechanical properties of the steel, such as impact toughness. Furthermore, the detailed TEM analysis underscores the complex interplay between tempering temperature and carbide evolution, emphasizing the necessity of precise temperature control during heat treatment to achieve the desired mechanical properties.

The influence of tempering temperature on the impact toughness of steel is shown in Figure 9.

 doi:10.20944/preprints202407.1112.v1

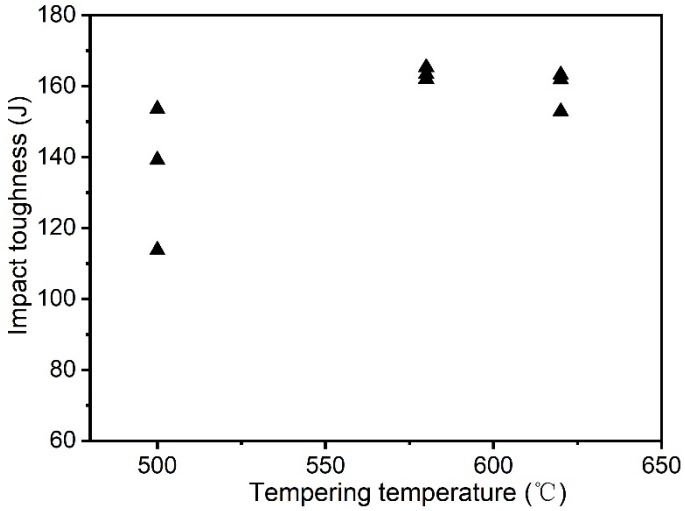

Figure 9. Impact toughness after tempering.

The impact toughness curve in Figure 9 reflects the evolution of carbides with increasing tempering temperature. Impact toughness increases, peaking at 580°C, and then decreases slowly at 620°C. The scatter in impact toughness values decreases with higher tempering temperatures, indicating improved material homogeneity. At 500°C, fine precipitates are oriented, as shown in Figure 3b, and low-angle boundaries are prevalent, as depicted in Figures 4a and 5b. This orientation of fine precipitates and high density of low-angle boundaries contribute to moderate impact toughness at this temperature. At 580°C, the carbide orientation decreases (Figure 3c), and the proportion of low-angle boundaries also diminishes (Figure 4b), leading to a peak in impact toughness due to the more random distribution of precipitates and the enhanced dislocation mobility. This results in reduced dispersion in impact toughness values, indicating more consistent mechanical properties. However, at 620°C, the impact toughness drops significantly due to the coarsening of carbides (Figure 7c). The larger, coarsened carbides provide less effective barriers to crack propagation, leading to a reduction in impact toughness. Additionally, the increase in high-angle boundaries at this temperature reduces the material's ability to absorb impact energy, further contributing to the decrease in toughness.

4. Conclusions

This study comprehensively investigates the influence of tempering temperature on the precipitation behavior, misorientation distribution, and impact toughness of high-nickel steel. The following key conclusions can be drawn:

(1) Tempering high-nickel steel at varying temperatures significantly affects the precipitation of carbides. At 500°C, fine carbides with a Widmanstätten distribution are prevalent. As the tempering temperature increases to 580°C, the carbides lose their crystallographic morphology and exhibit reduced dislocation density and increased spheroidization. At 620°C, significant coarsening of carbides occurs, with smaller precipitates dissolving and larger particles growing, leading to a more homogenous but coarser microstructure.

(2) The study reveals that low-angle grain boundaries decrease as tempering temperature increases. At 500°C, low-angle boundaries exceed 75%, but this proportion reduces to about 70% at 580°C and further decreases at 620°C. This reduction in low-angle boundaries correlates with the randomization of precipitate orientations and the reduction in dislocation density, enhancing the steel's impact toughness up to 580°C. However, at 620°C, the increase in high-angle boundaries and carbide coarsening negatively impacts the toughness.

(3) The impact toughness of the steel improves with tempering temperature, reaching a peak at 580°C, where the balance between fine, randomly distributed precipitates and reduced dislocation density optimizes mechanical properties. Beyond this temperature, at 620°C, the coarsening of

 doi:10.20944/preprints202407.1112.v1

carbides and the formation of high-angle grain boundaries diminish the impact toughness. This behavior underscores the critical importance of precise tempering temperature control to achieve the desired mechanical properties in high-nickel steels.

Declaration of Competing Interest: The authors declare that they have no known competing financial interests or personal relationships that could have appeared to influence the work reported in this paper.

Acknowledgments: The authors acknowledge financial support from Kunlun Talent Project of Qinghai Province.

References

1. Anatoliy Zavdoveev, Valeriy Poznyakov, Thierry Baudin,, et al. Effect of heat treatment on the mechanical properties and microstructure of HSLA steels processed by various technologies, Materials Today Communications,Volume 28,2021,102598,
2. Abdullah M R, Liang F, Hongneng C, et al.Computationally optimize microstructural investigation of austenitic steels for high strength-toughness properties[J].Journal of Materials Science, 2023.
3. Uskov, D. P. (2023). Properties of high-strength complex-alloy steel for casing pipes in cold-resistant and corrosion-resistant versions. *Steel in Translation, 53(10), 837-845.
4. S. Tekeli and A. Güral.Microstructural characterization and impact toughness of intercritically annealed PM steels[J].Materials Science and Engineering: A, 2005.
5. Jain A S, Mustafa M I, Sazili M I I M, et al.Effects of destabilization and tempering on microstructure and mechanical properties of a hypereutectic high-chromium cast iron[J].Journal of Materials Science, 2022, 57(32):15581-15597.
6. Pohjonen A, Babu S R, Visuri V V .Coupled model for carbon partitioning, diffusion, Cottrell atmosphere formation and cementite precipitation in martensite during quenching[J].Computational Materials Science, 2022, 209:111413-.
7. Wang H, Shen F,Yue WangFengkai YanZhiyuan ChangCansheng YuJian KangSebastian Münstermann.Effect of Tempering Temperature on the Microstructure, Deformation and Fracture Properties of an Ultrahigh Strength Medium-Mn Steel Processed by Quenching and Tempering[J].steel research international, 2023.
8. Du Y, Hu X, Zhang S, et al.Precipitation behavior of Cu-NiAl nanoscale particles and their effect on mechanical properties in a high strength low alloy steel[J].Materials Characterization, 2022:190.
9. Kawahara Y, Kaneko K, Sawada H, et al.Transition from carbon clusters to ε, θ-carbides in a quenched and aged low-carbon ferritic steel[J].Acta materialia, 2023.
10. Zeng T Y, Li W, Wang N M, et al.Microstructural evolution during tempering and intrinsic strengthening mechanisms in a low carbon martensitic stainless bearing steel[J].Materials Science and Engineering: A, 2022, 836:142736-.
11. Farber V M, Khotinov V A, Selivanova O V, et al.Evolution of the Structure and Mechanical Properties of Medium-Carbon Microalloyed Steel during High-Temperature Tempering[J].The Physics of Metals and Metallography, 2023, 124(8):824-830.
12. Hu J, Liu Y, Wang G, et al.Effect of Tempering Treatment on Microstructural Evolution and Mechanical Behavior of Heavy-Wall Heat Induction Seamless Bend Pipe[J].Materials, 2022, 15(1):259-.
13. Liu J, Wei S, Sun J, et al.Effect of Tempering Temperature on the Microstructural Evolution and Properties of 800 MPa Grade Low-Carbon Bainite-Deposited Metals[J].Metallurgical and Materials Transactions, A. Physical Metallurgy and Materials Science, 2022..
14. He B B, Guan Q W .Effect of Ausforming Strain on the Microstructural Evolution of Lath Martensite in Low Carbon Steel[J].Metals and Materials International, 2022.
15. Fang K, Guo X, Huang F, et al.Effects of alloying elements on the microstructure and mechanical properties of as-cast Cr12MoV cold-working die steel[J].International Journal of Materials Research, 2022(2):113.
16. Peng, G., Ye, G., Jun, C., Zhenyu, L., Yue, Z., & Guodong, S.** (2019). Study on Direct Quenching and Tempering Process of 1000MPa Grade Low Alloy High Strength Steel. *IOP Conference Series: Materials Science and Engineering, 677*(2), 022059.
17. 17 Park H, Seol J, Lim N, et al.Study of the decomposition behavior of retained austenite and the partitioning of alloying elements during tempering in CMnSiAl TRIP steels[J].Materials & Design, 2015, 82:173-180.
18. Zhang X, Liu H, Ren Y J, et al.A novel way refining the partially reverted globular austenite in reversion from martensite[J].ISIJ International, 2023.
19. Clarke A J, Miller M K, Field R D, et al.Atomic and nanoscale chemical and structural changes in quenched and tempered 4340 steel[J].Acta Materialia, 2014.
20. Xu P, Tomota Y, Oliver E C .Dynamic Recrystallization and Dynamic Precipitation Behaviors of a 17Ni–0.2C Martensite Steel Studied by In Situ Neutron Diffraction[J].ISIJ International, 2008, 48(11):1618-1625.

21. Conde F F, Ribamar G G, Escobar J D, et al.(113064)EBSD-data analysis of an additive manufactured maraging 300 steel submitted to different tempering and aging treatments[J].Materials Characterization, 2023:203.
22. Jiali,Zhang,Lutz, et al.Multi-probe microstructure tracking during heat treatment without an in-situ setup: Case studies on martensitic steel, dual phase steel and β-Ti alloy[J].Materials Characterization, 2016.
23. Zhang Y, Chang Q, Shao Y, et al.Assessment of the creep damage in HR3C steel using the misorientation parameters derived from EBSD technique[J].Materials Letters, 2022, 306:130893-.
24. Dobe R, Das A, Mukherjee R, et al.Evaluation of grain boundaries as percolation pathways in quartz-rich continental crust using Atomic Force Microscopy[J].Scientific Reports, 2021, 11(1):9831.
25. Dey S, Chatterjee S, Ritanjali S R, et al.Nanoscale visualization of high-angle misorientations in quartz-rich rocks using SEM-EBSD and Atomic Force Microscopy[J].Journal of Structural Geology, 2024, 183.
26. Jiang R, Zhang W, Zhang L, et al.Strain localization and crack initiation behavior of a PM Ni-based superalloy: SEM-DIC characterization and crystal plasticity simulation[J].Fatigue & Fracture of Engineering Materials and Structures, 2022(6):45.
27. Li C, Dubovi J, Klein C .Application of electron backscatter diffraction in facet crystalline orientation study of Al-Cu-Fe alloy[J].Materials Characterization, 2022:191.
28. Xu J, Brodin H, Peng R L, et al.Effect of heat treatment temperature on the microstructural evolution of CM247LC superalloy by laser powder bed fusion[J].Materials Characterization, 2022, 185:111742-.
29. Liang G, Tan Q, Liu Y, et al.Effect of cooling rate on microstructure and mechanical properties of a low-carbon low-alloy steel[J].Journal of Materials Science, 2021, 56(5):1-11..
30. Yaso M, Hayashi S, Morito S, et al.Characteristics of Retained Austenite in Quenched High Carbon-High Chromium Alloy Steels[J].Journal of the Japan Institute of Metals, 2009, 73(11):852-856.